Technical Report

Atom Probe Analysis of Fine Alloy Carbide in Steel – Determination of Chemical Compositions

Yukiko KOBAYASHI* Jun TAKAHASHI

Abstract

Atom probe tomography is a powerful technique for the quantitative investigation of fine precipitates owing to its sub-nanometer spatial resolution and excellent detection limits, which in principle allow for the measurement of all elemental species. However, in practice, various artifacts generated during measurement and data reconstruction have been reported, which can hinder data interpretation. In this study, we investigated the atomic ratio of carbon (C ratio) and its size dependence in nanometer-sized TiC precipitates in precipitation strengthened steel. The carbon ratio was determined for precipitates approximately 5 nm in diameter. However, for extremely fine precipitates smaller than 1.5 nm, accurate determination was difficult due to statistical errors arising from less than 100% detection efficiency and artifacts peculiar to dissolved solute C atoms.

1. Introduction

Fine alloy carbides such as TiC and NbC in steel materials are widely used in various high-strength steels because significant precipitation strengthening can be achieved by appropriately controlling their precipitation state. These carbides possess an NaCl-type structure and form plate-like precipitates in ferrite according to the Baker-Nutting orientation relationship. However, atom probe observations report that during the early precipitation stage, irregularly shaped "nanoclusters" or a "diffuse atmosphere" containing Fe atoms are generated.[1, 2] Conversely, in nitrides such as NbN and TiN, monolayer clusters have been observed.[1, 3] While these precipitation kinetics are crucial for alloy design and microstructure control, interest also extends to the composition of precipitates and its evolution, including precursor stages like clusters. Particularly during the initial precipitation stage, the free energy of the precipitate is significantly influenced by interfacial energy, potentially differing from the stable composition of the precipitated phase.

Atom probe tomography (abbreviated as 3DAP or APT) identifies the elemental species and three-dimensional position of individual atoms within a needle specimen using the phenomenon of field evaporation. They are characterized by sub-nanometer spatial resolution and excellent detection limits, and in principle, can measure all elemental species from light to heavy elements.[4, 5] Therefore, atom probe analyses are effective for investigating the composition of fine precipitates during the early stages of precipitation.

However, it has been reported that the measured data can exhibit distributions and concentrations that differ from those actually present in the specimen, associated with the measurement principles. These anomalies are often referred to as "artifacts," and in this paper, we also refer to the atomic distributions observed in the data that differ from the actual distribution as artifacts. To avoid mistaking these for the actual distribution, it is necessary to understand the measurement principles and the field evaporation mechanism when selecting experimental conditions and interpreting data.[5] Typically, the evaporation field varies by phase and further depends on the elemental species of solute atoms within it. Consequently, preferential evaporation or retention for specific elemental species produce an apparent concentration different from the actual concentration. Furthermore, the three-dimensional reconstruction parameters used to obtain atom maps are an approximation. For instance, when the evaporation field differs due to crystallographic orientation or elemental species on the tip surface of the needle specimen, the ion flight trajectory changes, causing aberrations known as trajectory aberration. A representative example is the Local Magnification Effect. Different phases with varying evaporation fields alter the local curvature of the needle specimen tip surface, changing the flight path and causing deviations from the actual atomic positions through 3D reconstruction. Furthermore, in the detector, the Pile-up Effect occurs when multiple ions arrive simultaneously in the vicinity on the detector, leading to ion counting loss. This also affects the

* Ph.D., Senior Researcher, Materials Characterization Research Lab., Advanced Technology Research Laboratories
20-1 Shintomi, Futtsu City, Chiba Pref. 293-8511

detected concentration. Furthermore, in the mass spectrum, ions with the same mass-to-charge ratios cause peak overlap. Therefore, considering isotope ratios, it is necessary to estimate the ratio of each ion within the peak. Furthermore, statistical errors in composition arising from the ion detection efficiency being less than 100% must be considered. While it is necessary to understand and use appropriate conditions under which quantitative analysis is achievable for the material, composition determination remains challenging due to the presence of the such issues described above.

Therefore, this study considers the challenges in quantitative measurement, to identify conditions under which atom probe quantitative analysis is feasible for steel materials. Based on this, we report on research that determined the chemical composition of fine TiC precipitates and investigated the composition dependence on precipitate particle size.

2. Quantitativeness of Alloying Elements in Steel[6)]

Properly evaporating all atoms constituting the needle sample is essential to achieve quantitative accuracy in atom probe analysis. However, slight differences in the evaporation field for each elemental species affect quantitativeness. Alloying elements added to iron alloys differ from atoms in pure metals because they are surrounded by iron atoms, resulting in different evaporation fields compared to pure metals. Therefore, experiments were conducted using ferrite model alloys containing representative alloying elements added to steel materials. The quantitativeness was investigated by varying experimental conditions, such as specimen temperature, for the atom probe analysis.

Figure 1 shows the specimen temperature dependence of apparent composition to chemical composition of the alloying elements, expressed as ratios. A vertical axis value of 1 indicates correct detection. At lower specimen temperatures, the detected composition was closer to the actual alloy composition, but the deviation increased significantly as the specimen temperature increased. Elements that evaporate more readily than Fe (preferential evaporation) were detected at lower concentrations than their actual composition, while elements that evaporate less readily than Fe (preferential retention) were detected at higher concentrations than their actual composition. This trend revealed the order of ease of evaporation in the iron matrix: Cu > Cr > Mn ~ Mo > Fe > Ti ~ Si.

Comparing with the binary phase diagram with Fe, elements showing phase separation with Fe exhibit preferential evaporation, elements forming complete solid solutions with Fe exhibit neither preferential evaporation nor retention, and elements forming intermetallic compounds with ordered structures exhibit preferential retention. This trend corresponds to the bonding strength between Fe atoms and the dissolved solute atoms.

This experiment was conducted at a low pulse repetition rate (1.5 kHz), resulting in a long DC voltage application time between pulses, which accentuates preferential evaporation and retention. Although modern atom probe instruments operate at high pulse repetition rate(> 20 kHz), making preferential evaporation and retention less apparent,[7)] this phenomenon is still present and may appear strongly depending on the material and experimental conditions.

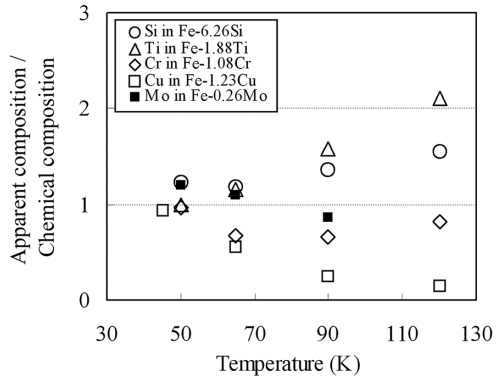

Fig. 1 Specimen temperature dependence of apparent composition to chemical composition of the alloying elements[6)]

3. Anomalous Distribution of Dissolved Carbon in Atom Map Due to Ferrite Crystallographic Orientation[8)]

Carbon (C), the most important alloying element in steel materials, exhibits a phenomenon in atom probe analysis where its atomic position significantly differs from its actual location. This complicates the quantification of fine precipitates and segregating atoms in atom probe analysis.

Figure 2 shows 3D atom maps of C and Fe atoms in ferritic steel, martensitic steel, and spheroidized cementite in annealed pearlitic steel, along with field ion microscope (FIM) images. While dissolved C should be uniformly distributed in ferritic steel, the atom map shows C atoms distributed non-uniformly along the measurement direction. In contrast, the atom maps of martensitic steel and spheroidized cementite showed uniform C distribution without any gradation. While no distinct contrast was observed in martensite and cementite in the FIM images, a clear contrast corresponding to crystallographic orientation was observed in ferrite. This suggests a relationship between FIM contrast and C distribution in an atom map.

Figure 3(a–c) shows the FIM image of ferritic steel, the corresponding C atom map (xy-plot) observed from the needle specimen front at a wide angle, and the 2D concentration profile of C. C atoms are enriched in {002}, {112}, and {222} crystallographic poles and the zone lines connecting them, while they are depleted around the 011 pole. The enriched C atom locations correspond to the dark regions in the FIM images. The maximum local C concentration was

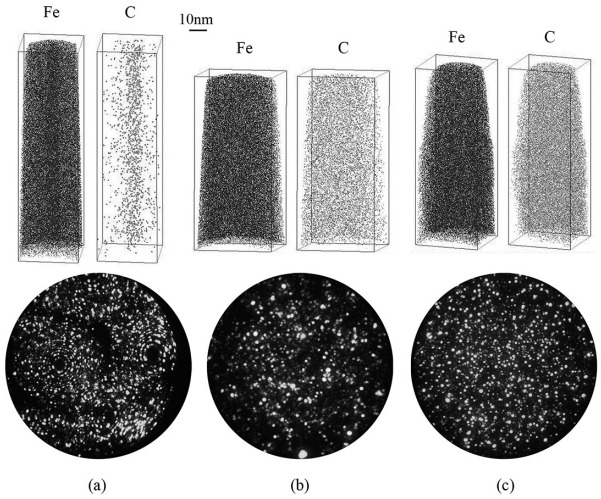

Fig. 2 C, Fe atom maps and FIM images of (a) ferritic steel, (b) martensitic steel and (c) spheroidized cementite[8)]

close to 1 at% at the 112 pole, while the minimum was below 0.1 at% around the 011 pole. Note that the actual dissolved C concentration in this steel is approximately 0.15 at%. Such pronounced concentration localization (enrichment) was observed only for the dissolved C atoms in the ferritic steel and hardly occurred for the other alloying elements Mn and Al. These were considered to be artifacts caused by either surface diffusion of C atoms on the needle specimen surface (Field induced migration) or differences in the trajectory aberration between Fe and C atoms. This phenomenon has also been reported for other light elements (N, P), and efforts are underway to elucidate the mechanism and develop countermeasures.[9)]

On the other hand, the dependence of cementite C detection composition on experimental conditions have been investigated separately, confirming that quantitative results can be obtained with appropriate experimental conditions and mass assignment.[10, 11)]

4. Composition Determination of Fine TiC Precipitates in Ferritic Steel[12)]

Recognizing the issues in atom probe analysis described above, we addressed the challenge of determining the composition of fine TiC precipitates and elucidating their size dependence. The steel used for observation was the TiC-precipitated ferritic model steel described in Reference[13)], with the precipitate size varied by the isothermal aging time at 580°C. After considering the factors affecting atom probe analysis that influence C composition determination, we first determined the composition of TiC precipitates with a sphere equivalent diameter of approximately 5 nm, then investigated finer TiC precipitates.

4.1 Composition of 5 nm precipitates

Figure 4 shows an atom map containing TiC precipitates with a sphere equivalent diameter of approximately 5 nm. Since the TiC phase has a higher evaporation field than the ferrite phase,[14, 15)] the local magnification effect tends to elongate the precipitates in the lateral direction. This elongation is particularly pronounced for C atoms, exhibiting greater trajectory aberration than Ti atoms. Additionally, C atoms are sometimes observed trailing behind the precipitation particles, suggesting the possibility of preferential retention of C atoms. Figure 4(b) shows an atom map cropped around the 10 nm-sized precipitat indicated by the arrow in Fig. 4(a). The number of Ti and C atoms was compared before cluster analysis (Fig. 4(b)), which includes surrounding solid solution atoms, and after cluster analysis using the Maximum separation method (Fig.4(c))[16)]. The error caused by the presence of C atoms displaced outward due to aberration, resulting in a slightly lower estimate than the actual value, was approximately 0.01 for C/(C+Ti) (C ratio, calculated by number of C and Ti atoms). This error magnitude is smaller than the variation in C ratio among the precipitate particles described later, making its influence negligible.

Next, we estimated the impact of detection loss of ions due to the pile-up effect in the detector. Since detection loss of C ions has been reported in atom probe analysis of carbides,[14)] we investigated

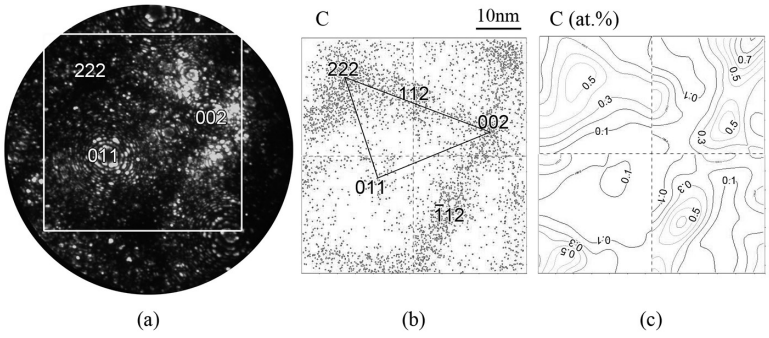

Fig. 3 (a) FIM image of ferritic steel and (b) corresponding front view (xy-plot) of carbon atom map toward the depth direction of the specimen. Note that four analyses provided with various tilt angles are combined. (c) 2D concentration profile of carbon corresponding to (b).[8)]

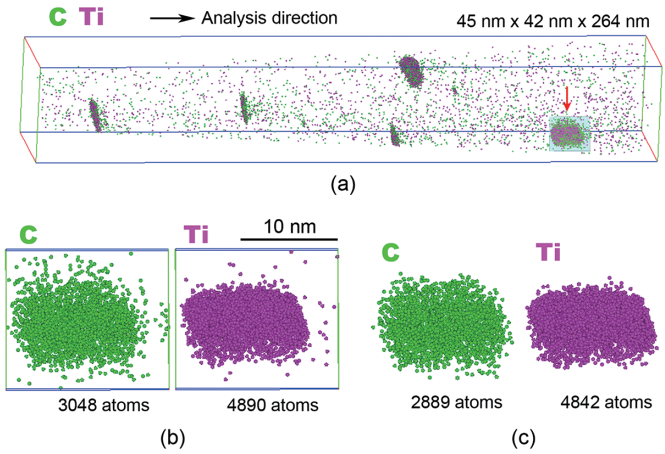

Fig. 4 (a) Elemental map of the steel aged for 512 h, (b) selected region around the largest TiC particle indicated by red arrow before cluster analysis and (c) after cluster analysis.[12)]

Table 1 C ratio in the four TiC particles in the mass assignment before and after peak deconvolution[12)]

	C/(C+Ti) ratio				
	Particle 1	Particle 2	Particle 3	Particle 4	Total
Before peak deconvolution	0.374	0.379	0.389	0.370	0.377
After peak deconvolution	0.380	0.416	0.397	0.404	0.396

this using isotope ratio changes,[17)] but the results indicated the detection loss of C in the TiC precipitates was minimal. Considering the peak overlap of Ti^{2+} and C_2^+ ions in the mass spectrum, we estimated the composition of the 5 nm TiC precipitates by correcting for this overlap by peak deconvolution of Ti and C using the isotope ratio. **Table 1** shows the C ratios for four representative TiC precipitates. The C ratio before peak deconvolution was 0.38±0.01, while after peak deconvolution it was 0.40±0.02. The reason the C ratio variation increased after peak deconvolution was due to larger errors resulting from estimation based on the less abundant isotope. Considering the above all issues, it was concluded that the C ratio of the TiC precipitates, with a sphere equivalent diameter of approximately 5 nm, is 0.40±0.02. Similarly, using an NbC precipitation model steel prepared in the same manner, the C ratio of the NbC precipitates was determined to be 0.45±0.05. In both cases, the results showed that C has fewer atoms than the alloying elements. The fact that C has fewer atoms than Ti implies the presence of C vacancies, suggesting the possibility of hydrogen trapping at the precipitate interface.[18)]

4.2 Composition of precipitates approximately 1 nm in size

For smaller precipitates, the limited number of constituent atoms precludes the application of C composition correction via peak deconvolution, as performed for the approximately 5 nm diameter precipitates. **Figure 5** shows the Ti atom maps for the steels after 580°C aging for 1 h and 2 h, along with the C ratio versus TiC precipitate size (white circles). The C ratio converged significantly when the precipitation size exceeded 10 000 atoms (equivalent to a spherical particle diameter of ~5 nm), whereas it showed large variations at smaller sizes. We discussed whether the observed variation in C ratio and the size dependence of the mean value represents the actual values.

The plots and error bars shown in red in Fig. 5 represent the mean and standard deviation of the C ratio calculated for approximately 30 precipitate particles in size order. The mean C ratio remained nearly constant for precipitate sizes of 200 atoms or larger (equivalent to a spherical diameter of ~1.5 nm), but gradually decreased below this size. Furthermore, calculating the statistical error in the C ratio expected from the ion detection efficiency (35% in this experiment) within the observed size range revealed a clear increase with decreasing size. This suggests that statistical error is the primary reason for the larger standard deviation observed in smaller precipitates in this experiment. However, the reliability of the observed decrease in the mean value cannot be fully confirmed due to the large variation in C ratios among individual precipitate particles. Furthermore, examining atom maps for precipitates below 1.5 nm diameter revealed the influence of the aforementioned artificial enrichment of dissolved C atoms depending on crystallographic orientation on the detected composition of the precipitates. Based on these results, it was concluded that reliable composition determination for TiC precipitates around 1 nm in size is difficult due to statistical error caused by detection efficiency less than 100% and the artificial C enrichment in atom maps.

5. Conclusion

This paper reports fundamental research for applying atom probe tomography to steel materials, covering the detection and quantification of alloying elements in steel, the artifacts in detecting dissolved carbon associated with ferrite crystallographic orientation, and attempts to determine the composition of fine alloy carbide precipitates in ferritic steel. The C ratio in TiC precipitates was determined for precipitates of 5 nm in diameter, but for finer precipitates, reduced reliability due to statistical error and the artificial enrichment in detecting dissolved carbon hindered the determination of the C ratio.

Furthermore, even today, the detection accuracy of C atoms in

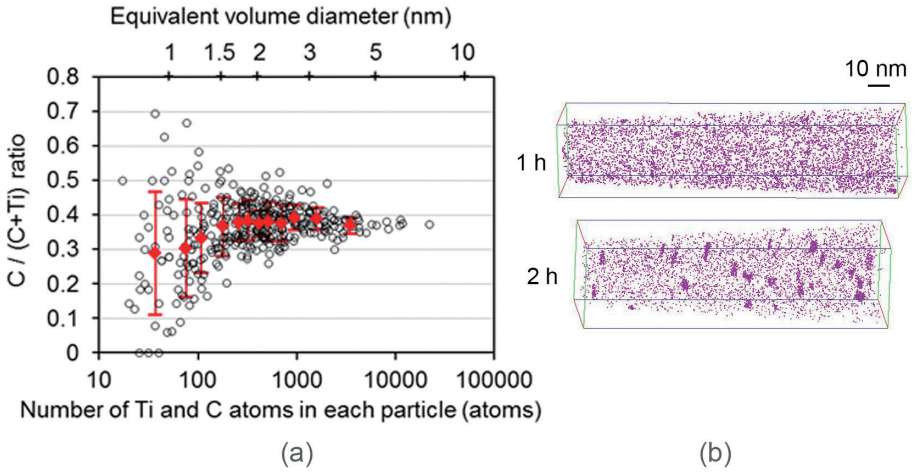

Fig. 5 (a) Observed each C ratio (white circle) and mean C ratio (red diamond) of TiC particles as a function of the total number of C and Ti atoms in each TiC particle analyzed using the atom probe. The number of solute atoms in each particle was estimated by dividing the detected number of C and Ti atoms by the nominal detection efficiency (0.35).[12)]
(b) Ti atom maps of steels aged for 1 h and 2 h.[13)]

alloy carbides remains a subject of debate. To improve accuracy, fundamental efforts are needed to investigate experimental condition dependencies using bulk samples with known concentrations or relatively large precipitates.[19–21)]

Although atom probe tomography is an effective technique for analyzing fine precipitates in steel materials, there are issues such as trajectory aberrations, quantitativeness, and atomic counting errors. These phenomena inherent to the measurement principles and the limitations should be understood to utilize this technique.

References

1) Danoix, F., Bémont, E., Maugis, P., Blavette. D.: Adv. Eng. Mat. 8 (12), 1202 (2006)
2) Wang, J., Weyland, M., Bikmukhametov, I., Miller, M.K., Hodgson, P.D., Timokhina, I.: Scripta Mater. 160 (2), 53 (2019)
3) Jack, D.H.: Acta Metall. 24 (2), 137 (1976)
4) Hono, K.: Bull. Iron Steel Inst. Jpn. 4 (7), 474 (1999)
5) Miller, M.K.: Atom Probe Tomography, Analysis at the Atomic Level. New York, Kluwer Academic/Plenum Publishers, 2000
6) Yamaguchi, Y., Takahashi, J., Kawakami, K.: Ultramicroscopy. 109 (5), 541 (2009)
7) Miller, M.K., Russell, K.F.: Surf. Interface Anal. 39 (2–3), 262 (2007)
8) Kobayashi, Y., Takahashi, J., Kawakami, K.: Ultramicroscopy. 111 (6), 600 (2011)
9) Gault, B., Danoix, F., Hoummada, K., Mangelinck, D., Leitner, H.: Ultramicroscopy. 113 (2), 182 (2012)
10) Takahashi, J., Kawakami, K., Kobayashi, Y.: Ultramicroscopy. 111 (8), 1233 (2011)
11) Takahashi, J., Kawakami, K., Kobayashi, Y.: Microsc. Microanal. 26 (2), 185 (2020)
12) Kobayashi, Y., Takahashi, J., Kawakami, K. Hono, K.: Microsc. Microanal. 27 (1), 1 (2021)
13) Kobayashi, Y., Takahashi, J., Kawakami, K.: Scripta Mater. 67 (10), 854 (2012)
14) Thuvander, M., Weidow, J., Angseryd, J., Falk, L.K.L., Liu, F., Sonestedt, M., Stiller, K., Andrén, H.-O.: Ultramicroscopy. 111 (6), 604 (2011)
15) Tsong, T.T.: Surf. Sci. 70 (1), 211 (1978)
16) Vaumousse, D., Cerezo, A., Warren, P.J.: Ultramicroscopy. 95, 215 (2003)
17) Angseryd, J., Liu, F., Andrén, H.-O., Gerstl, S.S.A., Thuvander, M.: Ultramicroscopy. 111 (6), 609 (2011)
18) Takahashi, J., Kawakami, K., Kobayashi, Y., Tarui, T.: Scripta Mater. 63 (3), 261 (2010)
19) Thuvander, M., Shinde, D., Rehan, A., Ejnermark, S., Stiller, K.: Microsc. Microanal. 25 (2), 454 (2019)
20) Jakob, S., Thuvander, M.: Microsc. Microanal. 30 (6), 1163 (2024)
21) Schiester, M., Waldl, H., Hans, M., Thuvander, M., Primetzhofer, D., Schalk, N., Tkadletz, M.: Surf. Coat. Technol. 477, 130318 (2024)

Yukiko KOBAYASHI
Ph.D., Senior Researcher
Materials Characterization Research Lab.
Advanced Technology Research Laboratories
20-1 Shintomi, Futtsu City, Chiba Pref. 293-8511

Jun TAKAHASHI
Dr. Eng., Principal Researcher
Advanced Technology Research Laboratories